



## Study of tablet-coating parameters for a pan coater through video imaging and Monte Carlo simulation

Bhoja Kandela<sup>a</sup>, Uday Sheorey<sup>b</sup>, Asish Banerjee<sup>c</sup>, Jayesh Bellare<sup>a,b,\*</sup>

<sup>a</sup> Department of Chemical Engineering, Indian Institute of Technology-Bombay, Mumbai 400076, India

<sup>b</sup> Department of Biosciences & Bioengineering, Indian Institute of Technology-Bombay, Mumbai 400076, India

<sup>c</sup> Gansons Ltd., Akbar Camp Road, Sandoz Baug, Kolshet, Thane 400607, India

### ARTICLE INFO

#### Article history:

Received 19 August 2009

Received in revised form 22 April 2010

Accepted 22 July 2010

Available online 4 August 2010

#### Keywords:

Pan coating

Tablet movement

Video imaging

Monte Carlo simulation

Coating variability

### ABSTRACT

The movement of tablets in a pan coater and the exposure of different surfaces of tablets for deposition of coatings by spray-coating have been studied by video imaging and Monte Carlo simulation techniques. A representative variety of tablets of different shapes and sizes were used at different pan loads and at various pan speeds. A single “tracer” tablet was used to track the motion of tablets and coating variables such as circulation time, surface time, projected surface area and surface velocity of a tablet were determined from the video imaging experiments. The coating uniformity is described in terms of the coating variation from tablet to tablet CV(tt) and a new parameter CV(st) the coating variation on a single tablet. The effect of shape of tablets on coating uniformity was analyzed by introducing a “sphericity” of tablet ( $\varphi_s$ ) into the CV models. The methodology, new models and the analysis developed here incorporating the additional parameters will help users to optimize the coating process in pan-coating operations.

© 2010 Published by Elsevier B.V.

### 1. Introduction

A pan coater is a widely used equipment in the pharmaceutical industry for the coating of medicinal tablets. A crucial requirement of pan coating is the uniformity of coating on all surfaces in the shortest time, particularly on the edges and sides of non-spherical tablets. Thus an understanding of all pan-coating parameters that govern the movement and coating of tablets are important for coating uniformity. There are many process parameters responsible for variability in the coating thickness. With much better control over most of these variables, such as the flow and uniformity of spray of the coating material, attention has shifted to the other variables of the pan-coating process and how to achieve the uniform coating on a variety of tablets and the highest possible rate of coating.

The coating uniformity is described in terms of two coating variations (CVs): CV(st) the coating variation on a single tablet and CV(tt) the coating variation from tablet to tablet. If either the CV(st) or the CV(tt) is high, a longer time will be required in order to achieve a uniform coating on tablets. The variations in coating thickness are due to the following process parameters:

- a) The variations in the circulation time, surface time, surface velocity, centroid location and projected area.

- b) The variations in the spray parameters and spatial non-uniformity of the spray flux distribution across the tablet bed.
- c) The design of the drum and the shape, size, location and number of baffles.

A variety of approaches have been used in the past by other authors to understand one or more aspects of these issues [1–5]. In the present study a production-coater was used and we have concentrated on a) while b) and c) are held constant, i.e., on the dynamics of the movement of the tablets. Our objective was to elucidate the effect of operating conditions such as the pan speed, pan load, tablet shape and tablet size on CVs in order to achieve uniform coating of tablets for a given spray flux. We utilized a video imaging technique and a tracer tablet to capture the movement of tablets as used by several others earlier [6–8]. In each run, we used a number of different tablets having representative shapes and sizes as actually used in the local pharma industry, together with one tracer tablet. Further, we carried out Monte Carlo simulations to calculate the CVs as a function of the pan-operating conditions as also done earlier by others [9–11]. We carried out actual coating experiments on a small number of tablets to measure the typical weight gain on tablets. To analyze the movement and orientations of these tablets, however, a novel colouring scheme was used for the tracer tablet to track and to record the tablet movements. The recorded movement of the tracer tablet was then used to calculate the circulation time, the surface time, the velocity and the projected surface area of the tablets. Furthermore, in order to understand the effect of shape of tablets, we have introduced a new parameter  $\varphi_s$ , the “sphericity” of the tablet, into the expressions for

\* Corresponding author. Department of Chemical Engineering, Indian Institute of Technology-Bombay, Mumbai 400076, India. Tel.: +912225767207; fax: +9122 25726895, +9122 25723480.

E-mail address: [jb@iitb.ac.in](mailto:jb@iitb.ac.in) (J. Bellare).

the velocity of and for CVs. Sphericity is the ratio of the surface area of an equivalent sphere to the surface area of the tablet.

Even though many people in the past have tried to understand the pan-coating process through different approaches, reviewed recently by Turton [12], there is still a lack of information as to how to optimize the coating process especially with respect to tablet shape. Muller and Kleinebudde [8] presented data on the tablet velocity for a number of different shapes. However, no one has studied CV(st), an important parameter for achieving a uniform coating on individual tablets. The current work investigates the effect of tablet shape on tablet velocity and also on CVs.

## 2. Experiments

### 2.1. Experimental set-up

A rotating-drum pan coater was used for the experiments (600 mm in diameter, model GAC-600, manufactured by Gansons Ltd., Thane). This is shown schematically in Fig. 1. A small CCD video camera (Wat-221S, CS mount, RGB video output, 25 fps; with a varifocal lens – Avenir CCTV lens, F/1.4, focal length 3.5–8.0 mm) was clamped to a horizontal mounting rod inside the drum in place of the spray guns. It was focused on the bed of tablets and its field of view covered the total spray region. Illumination of the tablet bed was provided by an external light source above the perforated drum. Using a short exposure time (250  $\mu$ s) we were able to capture images of the moving tablets without blur.

The rotational speed could be adjusted continuously from 3 to 30 rpm. Six “rabbit-ear” baffles were fitted inside the drum so as to thoroughly mix and tumble the tablets as the drum rotates. Only this shape and type of baffle were used in this study as they have been shown to ensure uniformity of mixing and tumbling in the least time as compared to tubular and ploughshare baffles [13].

The spray region is taken to be an elliptical area and lies totally within the scan area of the video camera, called the region of interest (ROI). These are shown schematically in Fig. 2.

### 2.2. Materials

The materials used in this project are separate lots of realistic tablets each of a different shape, size and mass. The base colour of all tablets was white so all the tablets were pre-coated with a dark colour in a separate operation, except for a few tablets of each lot which were left uncoated so that they could be used as tracer tablets in the bed of equivalent dark-coloured tablets. Four types of tablets in all were used in this investigation to evaluate the effect of shape and size of tablets

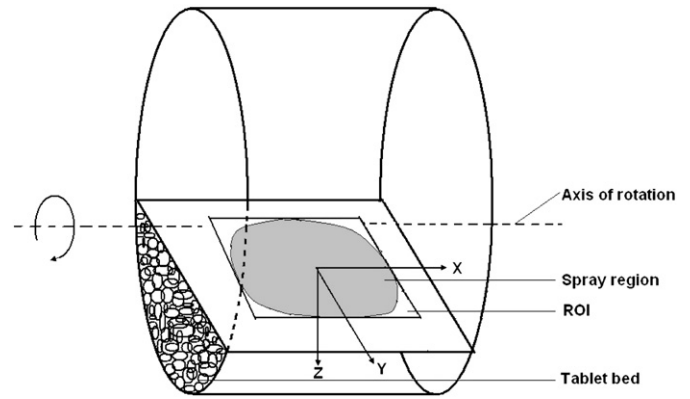


Fig. 2. A schematic of pan coater drum illustrating the axis of rotation of the drum, the stationary bed of tablets, the region of interest (ROI) viewed by the video camera, the elliptical spray region within this and the coordinate axes.

(see Table 1). All tablets are described in terms of a characteristic dimension  $D$  and the sphericity  $\phi_s$ .

In order to determine the actual weight gains of a variety of tablets, experimental runs were carried out in a separate but equivalent drum-coater using the same type of spray guns and coating material (HPMC) as used routinely for production.

### 2.3. Experimental procedure

The frame by frame motion of one white tracer tablet placed amongst dark-coloured tablets of the same shape, size and mass was captured by the video camera and a frame-grabber unit (Plextor, PX-M402U). This unit digitizes and downloads the video signals into a computer. The images are thereafter analyzed frame by frame by an image analysis code developed by us. The input image is converted into numerical values corresponding to the RGB values of each pixel. The code first confirms whether the tracer is present in each frame or not. Then the program counts the number of pixels having a white tracer tablet and calculates the centroid of the tracer tablet and the cross-sectional area of the tracer tablet. The code was first tested by conducting two runs, a) without the white tracer tablet in the pan coater so as to verify that the code did not register any false tracer tablet sightings, and b) that the code is able to differentiate the all-white tablet clearly from any reflections from the edges of the somewhat shiny dark-coloured tablets. The output of the image analysis code was analyzed in MATLAB® so as to derive the required data of response variables such as circulation, surface time, projected

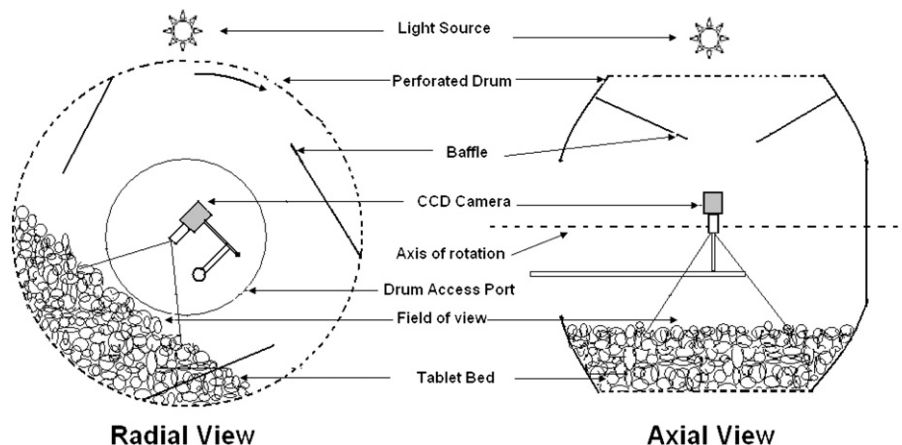

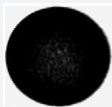
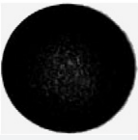




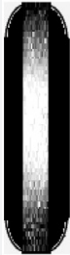


Fig. 1. A schematic of a typical perforated pan coater drum.

**Table 1**  
Shapes and sizes of the various tablets used in our experiments.

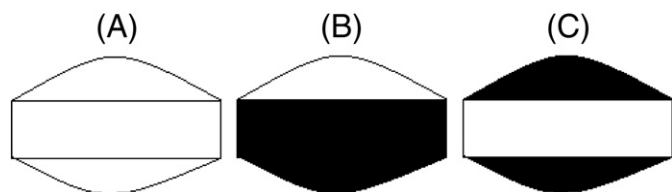
Shape/parameter	Small (D = 8.05 mm)	Medium (D = 9.85 mm)	Big (D = 11.95 mm)	Oblong (D = 18.01 mm)
Common name	Circular bi-convex	Circular bi-convex	Circular bi-convex	Oblong bi-convex
Top view				
Side view				
Diameter (d)	0.85 mm	9.85 mm	11.95 mm	$i = 7.67$ mm, $j = 18.01$ mm
Total thickness (T)	4.17 mm	4.65 mm	5.5 mm	6.15 mm
Side thickness (H)	3.19 mm	2.66 mm	3.08 mm	4.26 mm
Total surface area	184.01 mm <sup>2</sup>	241.47 mm <sup>2</sup>	349.14 mm <sup>2</sup>	497.36 mm <sup>2</sup>
Top surface area	116.76 mm <sup>2</sup>	79.45 mm <sup>2</sup>	51.69 mm <sup>2</sup>	138.88 mm <sup>2</sup>
Side surface area	115.63 mm <sup>2</sup>	82.58 mm <sup>2</sup>	80.62 mm <sup>2</sup>	219.61 mm <sup>2</sup>
Sphericity ( $\psi_s$ )	0.8607	0.8584	0.8527	0.6852
Weight (W)	0.22 g	0.30 g	0.65 g	0.83 g

Where  $D$  is the characteristic dimension of the tablet,  $i$  is the length of the minor axis,  $j$  is the length of the major axis and bulk density of tablets is 3000 kg/m<sup>3</sup>.

area and velocity of tablet. All the reported parameter values were averaged over 3 min of a run to reduce the experimental error.

To analyze the motion of tablets, we developed an image-processing algorithm to identify the orientation and outline of the tracer tablet. Then one all-white tracer tablet of the same shape, size and mass as the rest of the tablets was placed in the given lot of dark-coloured tablets in the rotating drum. A highly contrasting colour was chosen so as to ensure that the outline of the tracer tablet could be clearly delineated and the cross-sectional area was not overestimated as a result of shadowing against the backdrop of the bed of tumbling tablets of similar dimensions. In order to identify each surface of the tracer tablet as it moves on the surface of the tablet bed, different colours were applied to each of the two sides and the edge of individual tracer tablets, as depicted in Fig. 3.

The analysis of tracer tablet motion was carried out with four types of tablets (three bi-convex in shape and one oblong-shaped), at three pan speeds (4, 8, and 12 rpm), for two pan loads (10 and 12 kg) and using three different tracer tablets (white tracer, white-top and white edge tracers). The average values of circulation time, surface time, total projected area per pass and surface velocity are calculated from the data of several runs during one experimental session. These values were then utilized to determine the coating variations from a Monte Carlo technique in the modeling part of this study described below.



**Fig. 3.** Schematic of the tracer tablets indicating the distinct and different colours or patterns applied to the various surfaces. A: all-white tracer, B: white-top tracer, C: a white-side tracer.

### 3. Modeling

#### 3.1. Determination of the coating variability using a Monte Carlo technique

To determine the CV(tt) and CV(st) for a pan coater using the Monte Carlo technique, our model requires two main inputs, the spatial movements of a tablet and the spatial distribution of the spray flux within the region of interest viewed by the video camera.

##### 3.1.1. Data from video imaging measurements

This information required about the tablet movement includes the velocity distribution of a tablet in two directions ( $X$  and  $Y$ ) as well as the distribution of the location of the centroid of the tracer tablet, the distribution of circulation times, the distribution of surface time and the distribution of projected surface area of tablets as they pass through the spray zone. In our model the tablet velocity along the  $Z$  direction is not taken into account because this video imaging technique is not able to track the tablet inside the bed of tablets.

##### 3.1.2. Input from spray dynamics

The flux distribution of the spray depends on several process parameters such as the make and type of spray gun, the shape and spread of the spray, the distance between the spray-gun nozzle and the tablet bed, the relative humidity, temperature and flow rate of the air between the spray gun and the tablet bed, the fluid flow properties of the coating material in the gun at the ambient temperature inside the pan, the atomizing air pressure and the number of spray guns used.

The spray flux  $S$  at any given point  $(x, y)$  within the spray region for the coating material (HPMC) having a dilution ratio (w/w) of 0.1 and a flow rate of 125 ml/min is given by Eq. A4 as (in the Appendix):

$$S(x,y) = \frac{1}{2\pi(195)(163)} \exp\left(\frac{-1}{2}\left(\frac{x^2}{195^2} + \frac{y^2}{163^2}\right)\right) \quad (1)$$

### 3.1.3. Monte Carlo algorithm

In our experiments the effect of the operating conditions on CVs was studied using Monte Carlo simulations at three different pan speeds, two pan loadings and with four types of tablets. The simulations utilize the data from video imaging measurements. The flow chart of the algorithm used to simulate the coating process using a Monte Carlo simulation is shown in Fig. 4. In brief, from the centroid-location distribution generated from the video imaging experiments, a random starting location of the tracer tablet is selected. The next tablet location is calculated by randomly selecting  $X$  and  $Y$  velocities from the experimentally obtained velocity distributions using Eqs. 2 and 3:

$$x(j+1) = x(j) + V_x dt \quad (2)$$

$$y(j+1) = y(j) + V_y dt \quad (3)$$

where  $y$  is the centroid  $Y$ -location (in the direction parallel to the cascading layer of tablets) of a tablet,  $x$  is the centroid  $X$ -location (in the direction perpendicular to the cascading layer flow in the plane of the cascading layer) of a tablet,  $dt$  is the time increment and  $V_x$  and  $V_y$  are the randomly chosen components of tablet velocities in the  $x$  and  $y$  directions (from [10]).

The tablet-wall collisions are considered to be perfectly elastic. The schematic showing the typical motion of the tablet within the ROI and accounting for the collision with the sidewall is shown Fig. 5. The time increment is 40 ms, which is the same as the time taken by the camera to record successive images. The projected surface area values were randomly chosen from the experimentally obtained projected surface area distribution.

The coating weight gain at a particular time interval is calculated according to Eq. 4:

$$m_{i+1} = m_i + (SA_{proj} dt) \quad (4)$$

where  $m_i$  is the weight gained by a tablet,  $A_{proj}$  is the projected surface area at each sighting of the tablet within the spray,  $S$  is the spray flux at the centroid location of the tablet and  $dt$  is the time increment. The spray flux  $S$  was calculated from Eq. 1. When the tablet is out of spray region, the time is incremented by the one circulation time so that tablet again comes into spray region. This cycle was repeated until the total time is equal to or greater than the total coating batch time. The above cycle was repeated for all the tablets and the weight gain of each tablet was calculated.

The  $CV(tt)$  is calculated using Eq. 5a (from [10]), and  $CV(st)$  is calculated from Eq. 5b:

$$CV(tt) = \frac{\sigma(tt)}{\mu(tt)} \times 100 \quad (5a)$$

$$CV(st) = \frac{\sigma(st)}{\mu(st)} \times 100. \quad (5b)$$

Here  $\sigma(tt)$  is the standard deviation of the coating weight gain distribution from tablet to tablet,  $\sigma(st)$  is the standard deviation of the coating weight gain per unit area distribution on a single tablet.  $\mu(tt)$  is the average coating weight gain distribution per tablet and  $\mu(st)$  is the coating weight gain distribution per unit area for one tablet.  $\mu(tt)$  is calculated using Eq. 6a (from [10]), and  $\mu(st)$  is calculated from Eq. 6b:

$$\mu(tt) = \frac{tG}{N} \quad (6a)$$

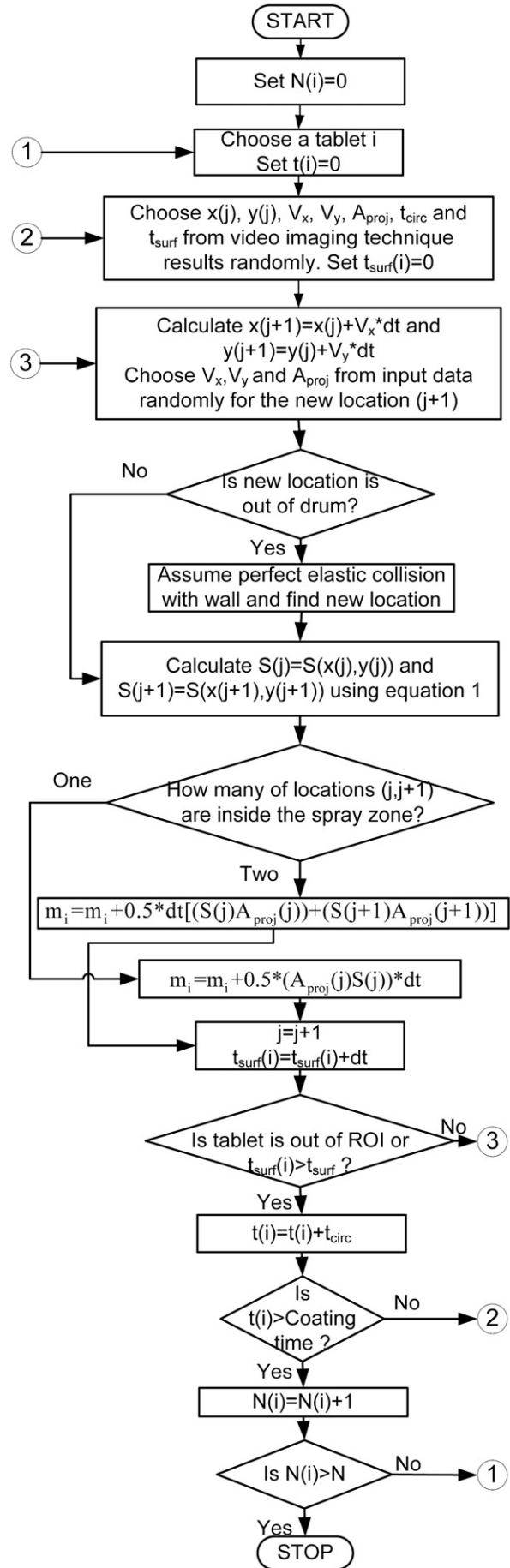


Fig. 4. The flowchart of the algorithm of the Monte Carlo method for calculating the coating variation (CV) from video imaging experiments.

(A) Typical tablet motion in ROI

(B) Motion of tablet accounting for a wall collision

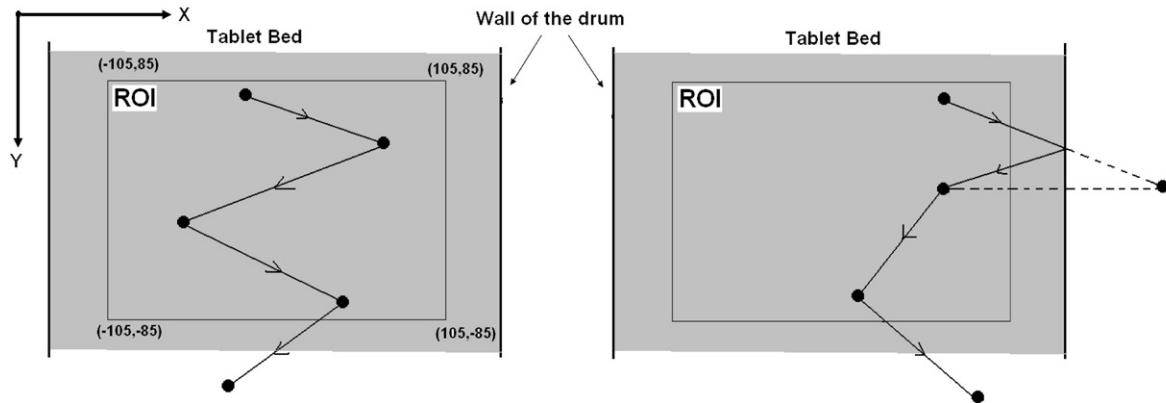


Fig. 5. The typical movement of a tablet through the spray region with and without collisions with the sidewall of the drum. (A) indicates the coordinates of the ROI within the spray region. (B) illustrates the possible motions of the tracer tablet after a collision with the sidewall.

$$\mu(st) = \frac{tG}{N} A_{total} \quad (6b)$$

where  $G$  is the mass flow rate,  $t$  is coating process time,  $N$  is the number of tablets and  $A_{total}$  is the total surface area of a single tablet.

4. Results and discussion

4.1. Results with tracer tablets with different patterns on various surfaces

Experiments using white tracer tablets which are depicted in Fig. 3 were carried out in order to elucidate the effect of operating conditions on response variables for different shapes and sizes of tablets.

4.1.1. Surface velocity ( $V_y$ )

The variation of the velocity for different sizes and shapes of tablets with pan speed is shown in Fig. 6, for 10 kg and 12 kg pan loads. The velocity of the tracer tablet increases with an increase in the pan speed because the kinetic energy supplied to the tablets increases. Oblong-shaped tablets ( $D=18.01$  mm) show a different velocity profile with pan speed compared to circular bi-convex tablets. For the tablets having a similar shape (circular bi-convex), the larger tablets ( $D=11.95$  mm) have less velocity than the smaller tablets

( $D=8.05$  mm). This is because for the same kinetic energy their velocity is less than for the smaller tablets. For a larger pan load, the inclination of the tablet bed increases and so the gravitational energy of the tablets at the top of the bed increases.

The surface velocity will also depend on pan diameter because the linear velocity ( $=R\omega$ ) varies with the pan radius ( $R$ ). The velocity of spherical particles (polystyrene spheres) in the cascading layer as a function of the particle diameter, pan diameter, pan speed and pan load was expressed by Muller and Kleinebudde [8] as:

$$\text{Model-1} : V_y = kR\omega^{2/3} \left(\frac{g}{d}\right)^{1/6} v^{1.8} \quad (7)$$

where  $V_y$  is the surface velocity of particle,  $R$  is the pan radius,  $\omega$  is the pan speed,  $d$  is the diameter of the particle,  $v$  is pan-load ratio (the ratio of the height of the tablet bed to the inside diameter of the drum of the pan coater) and  $g$  is the acceleration due to gravity. Muller and Kleinebudde [8] also provided information on tablet velocities and surface times for 3 sizes of tablets. However, the effect of the shape of the tablet on the surface velocity of the tablet was not considered in their investigations. Thus we modified the above Model-1 to take into account the effect

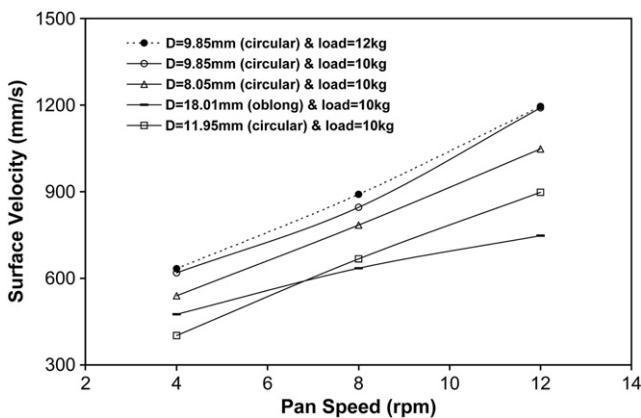


Fig. 6. Variation of the surface velocity of tablets (mm/s) as a function of pan speed for different shapes and sizes of typical tablets and pan loads.

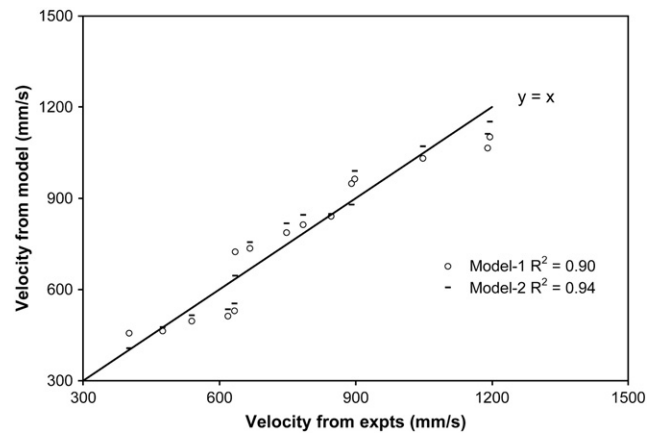


Fig. 7. Comparison of surface velocity (mm/s) for two models with the velocity determined by our video imaging experiments. Four tablets of different shapes and sizes were used in our experiments and there are 3 values for each (for the 3 different pan speeds).

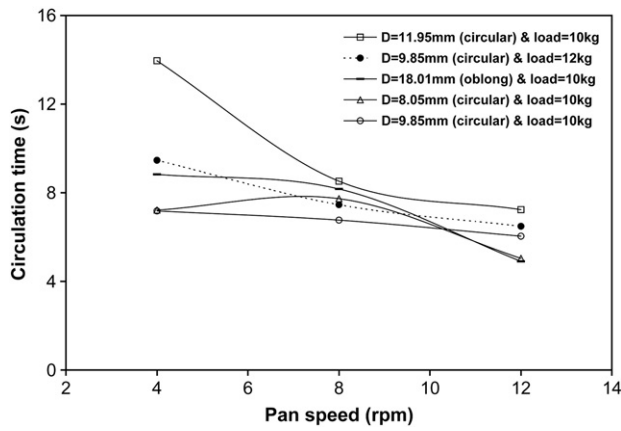


Fig. 8. The circulation time of tablets with pan speed, for different shapes, sizes and pan loads of tablets.

of the shape of tablets on the velocity of tablets by inserting a sphericity ( $\varphi_s$ ) term in Eq. 7, as shown in Eq. 8:

$$\text{Model-2} : V_y = 10.03R\omega^{2/3} \left(\frac{g}{D}\right)^{1/6} v^{1.8} \varphi_s^{0.7688} \quad (8)$$

Here  $D$  is characteristic diameter of the tablets and  $\varphi_s$  is our “sphericity” parameter. Then we plotted the calculated and experimental values and the  $R^2$  for the two models (1 and 2) and as shown in Fig. 7 we find that our model ( $R^2 = 0.94$ ) provides a better fit to the experimental values than Model-1 ( $R^2 = 0.90$ ), for a variety of tablets and pan speeds.

#### 4.1.2. Circulation time

As intuitively obvious, the circulation times of tablets generally decreases with increase in pan speed as the tracer tablet will come to the top of the bed within a shorter time. But the rate of decrease is a complex distribution for tablets of different shapes and sizes and pan loads, as shown in Fig. 8 for 2 typical pan loads. At the higher pan load, the circulation time of tablets was larger because the tracer tablet has to travel a larger distance within the bed.

#### 4.1.3. Surface time

The surface time was found to vary with the size and shape of tablets and pan loads. As the pan speed increases the velocity of tablets also increases, so each tablet spends less time within the ROI. For a similar shape of tablets the surface time is more for the larger tablets than for the smaller tablets, because a larger tablet has less

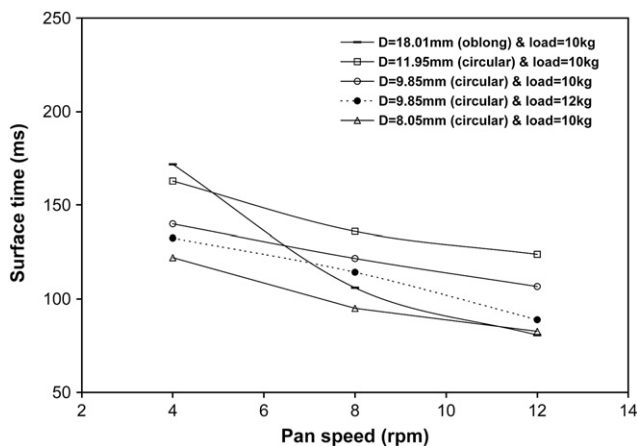


Fig. 9. The variation of surface time as a function of pan speed, for different shapes, sizes and pan loads of tablets.

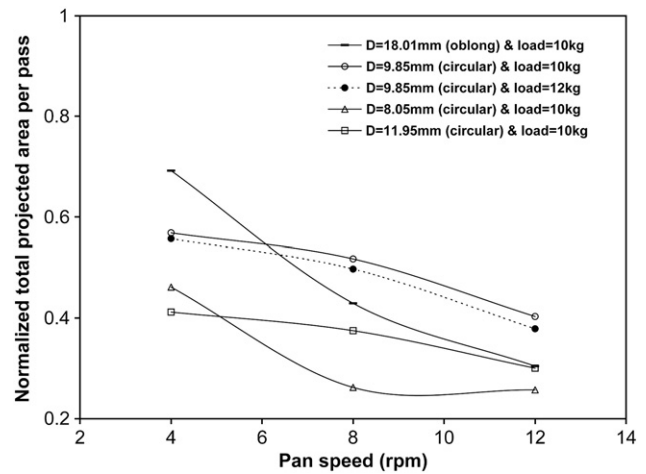


Fig. 10. The normalized total projected area per pass as a function of pan speed for different pan loads and tablets of different shapes and sizes.

velocity than a smaller tablet. As the pan load increases, the surface time of tablets was found to decrease because as the surface velocity of tablets increases the tablet spends less time within the ROI. The decrease of surface time with pan speed is more pronounced for capsule-shaped tablets than for the round shaped tablets and is shown in Fig. 9 for tablets of different shapes, sizes and pan loads.

#### 4.1.4. Total projected area per pass

The total area projected per pass varies with the tablet shape and its dimensions and decreases with increase in pan speed and pan loads. It is smaller for the smaller tablets ( $D = 8.05$  mm) than for the larger tablets (11.95 mm). It is more meaningful however to plot the variation of the normalized total projected area (the ratio of total projected area to the total surface area of the tablet) as a function of the pan speed rather than total projected area because the former is of dimensionless quantity. The normalized total projected area per pass decreases with pan speed and a larger pan load because the tablets spend less time within the ROI at higher pan loads and at higher pan speeds. This variation is depicted in Fig. 10 for different tablets and pan loads.

#### 4.1.5. Variations in coating thickness

A critical factor for the variation in coating thickness on tablets of different shapes other than spherical tablets is the dependence of the ratio of the side-projected-area to the top-projected-area. In order to

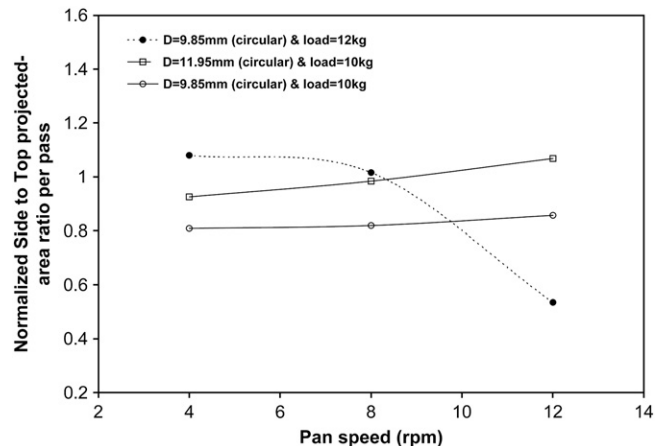
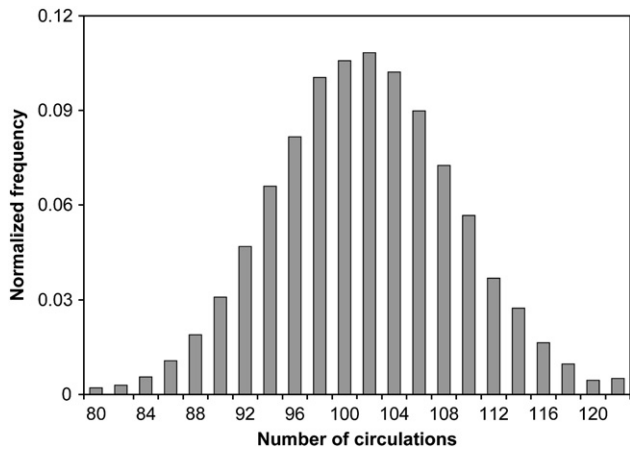


Fig. 11. The normalized side/top-projected area per pass as a function of pan speed and different pan loads for circular bi-convex tablets.



**Fig. 12.** The distribution of the number of circulations of a tablet over a period of 10 min of drum-rotation, simulated using the Monte Carlo technique. This is for circular bi-convex tablets (9.85 mm), at 8 rpm pan speed and a pan load of 10 kg.

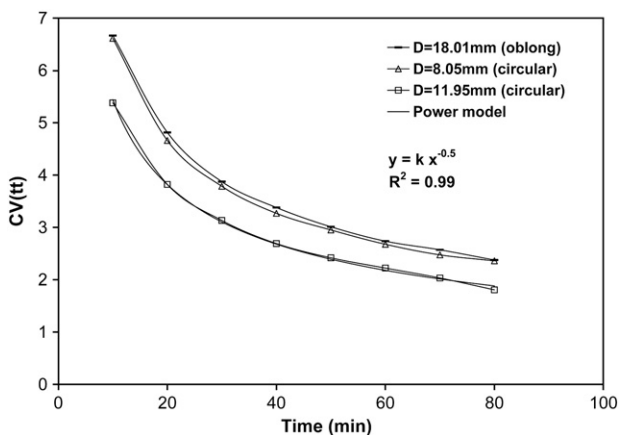
understand whether all the surfaces of the tablets are equally exposed to the spray flux and thereby would be uniformly coated or not we again used video imaging experiments to obtain this data. We used tracer tablets, as depicted in Fig. 3(B) and (C), having a different combination of colours on different surfaces – a white-top or a white-side, at three different speeds and at two pan loads. A white tracer tablet was utilized to find out CV(tt). Similarly the data from white-top and white-sided tracers was used for CV(st). The variation of the normalized ratio of side-projected area to the top-projected area at different pan speeds and for different tablet sizes and pan loads is shown in Fig. 11. A drastic change in the characteristic shape of the variation is seen as the pan load is increased.

4.2. Monte Carlo simulation of coating variations

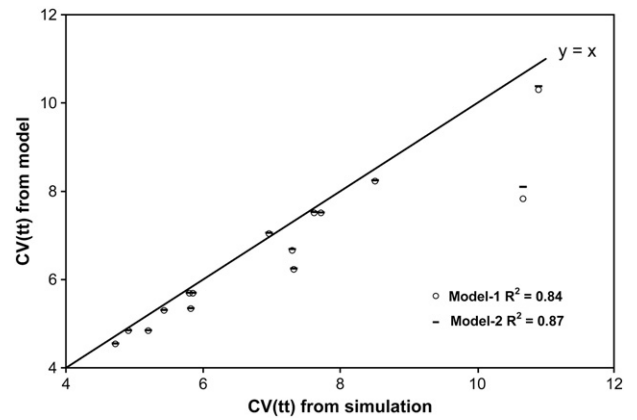
We have used the data generated from video imaging to study the distribution of CVs using the Monte Carlo modeling technique. A typical distribution of the number of tablet-circulations in the drum through the spray region is shown in Fig. 12.

4.2.1. Analysis of CV(tt)

In order to elucidate the dependence of CV(tt) on the coating process time, the coating process was simulated for different times (10 min to 80 min) using the Monte Carlo simulation technique. The



**Fig. 13.** The coating variation CV(tt) as a function of coating process time for different tablets, at 8 rpm speed and 10 kg pan load.



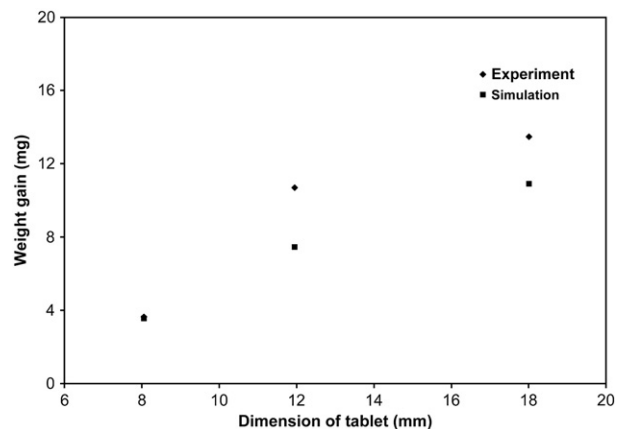
**Fig. 14.** Comparison of the coating variation CV(tt) determined from Monte Carlo simulation and from the two models, for a number of different tablets and pan loads. There are 3 points each for the 9.85 mm tablets at 10 kg load and at 12 kg load, 3 points for the 11.95 mm tablets at 10 kg load, 3 points for the 8.05 mm tablets at 10 kg load and 3 points for the 18.05 mm tablets at 10 kg load.

variation in CV(tt) with coating process time is illustrated in Fig. 13 for tablets of different shapes and sizes. The decrease of CV(tt) with increase in  $t$  is well fitted by a inverse power law, i.e., CV(tt) is proportional to  $t^{0.5}$ . The CV(tt) is larger for smaller tablets ( $D=8.05$  mm) when compared to larger tablets ( $D=11.95$  mm) of similar circular bi-convex shape, because  $N$  the total number of tablets is higher. For the larger oblong shape tablets ( $D=18.01$  mm) CV(tt) is much higher as compared to circular bi-convex tablets ( $D=11.95$  mm) because this shape has longer and sharper edges than the circular tablets. Even though the sphericity is high (0.85) the curve for smaller tablets (circular,  $D=8.05$ ) is close to the curve for  $D=18.01$ , because the total number of tablets of this smaller size ( $D=8.05$ ) is larger in a given pan load, leading to higher CV for the smaller tablet.

The dependence of CV(tt) on the operating parameters for a pan coater (the pan speed, pan load, tablet size, and coating time) has been given by Pandey et al. [10] as:

$$(\text{Model-1}) : CV(tt) = k \frac{d^{1.2} N^{0.5}}{\omega^{0.4} t^{0.5}} \tag{9}$$

where  $d$  is the particle diameter  $N$  is number of tablets,  $\omega$  is pan speed and  $t$  is the coating process time.



**Fig. 15.** Experimentally determined coating weight gain and that from Monte Carlo simulation, for tablets of different sizes.

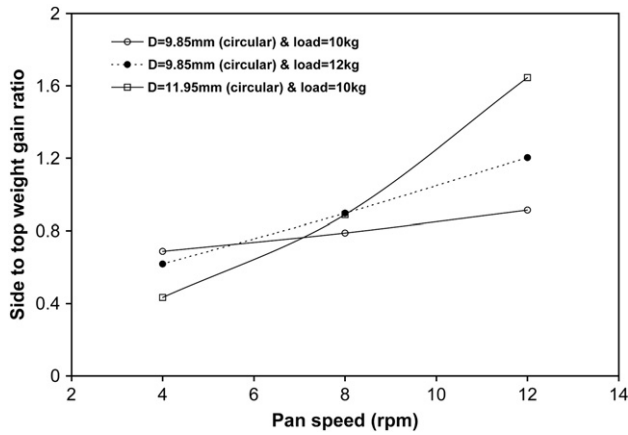


Fig. 16. Variation of the ratio of the side to top weight gain per unit surface area of tablets with pan speed, for various tablets, for two different pan loads of 10 and 12 kg.

To account for the shape of actual tablets, we introduce our “sphericity” parameter  $\varphi_s$  as shown in Eq. 10,  $D$  being the characteristic dimension of the tablet:

$$(\text{Model-2}) : CV(tt) = 2.84 \times 10^{-3} \frac{D^{1.2} N^{0.5}}{\omega^{0.4} t^{0.5} \varphi_s^{0.0127}} \quad (10)$$

We then compared the simulation values of  $CV(tt)$  for both models and calculated the  $R^2$  values for each, as shown in Fig. 14, for various tablets and pan loads. We note that our Model-2 incorporating the sphericity parameter is not a much better fit to the experimental data ( $R^2 = 0.87$ ) than Model-1 ( $R^2 = 0.84$ ), as the dependence of  $CV(tt)$  on sphericity ( $CV(tt) \propto \varphi_s^{-0.0127}$ ) is very less. As the  $CV(tt)$  does not have significant impact with sphericity any of two models can be used without any error.

We determined experimentally the actual weight gains of various tablets and compared these with simulation results as shown in Fig. 15, for three types of tablets ( $D = 8.05$  mm,  $D = 11.95$  mm and  $D = 18.01$  mm). It is observed that the simulation results are able to predict the experimental weight gain.

To determine the experimental result of coating variation  $CV(tt)$  is very difficult, as the weight gain of individual tablet should be known to find the variation between them.  $CV(tt)$  is not verified in this current work as the  $CV(tt)$  is calculated using the video imaging

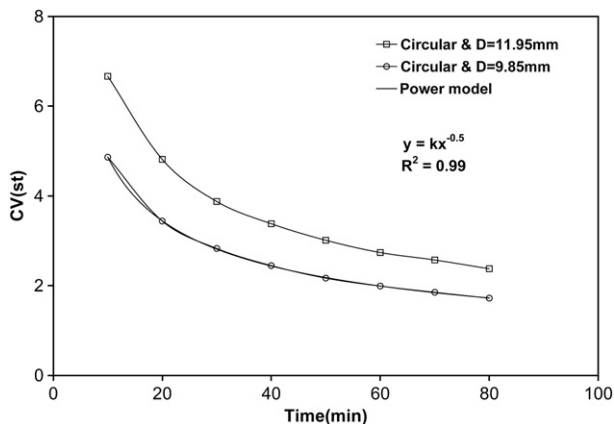


Fig. 17. The reduction of coating variation of a particular tablet  $CV(st)$  with increasing coating time, for tablets of two different sizes, at 8 rpm speed and a pan load of 10 kg.

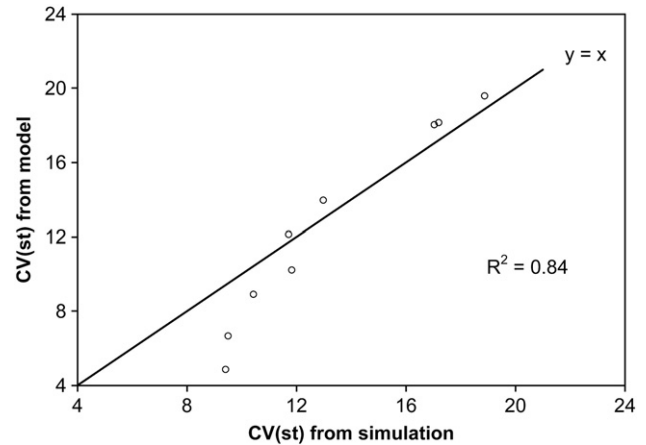


Fig. 18. The comparison between  $CV(st)$  from the model and from simulation.

experiment data and this method is already verified by Pandey et al. [10].

#### 4.2.2. Analysis of coating variation on a single tablet $CV(st)$

To achieve a uniform coating on a particular tablet the ratio of side-weight-gain to top-weight-gain ratio should be unity. To analyze and understand  $CV(st)$ , we calculated separately the coated weight gain of the top-surfaces and side-surfaces of tablets by the Monte Carlo simulation and from video imaging experiments, using the data on white-top and white-side tracer tablets. These values, shown in Fig. 16, are calculated for three pan speeds (4, 8 and 12 rpm) and two pan loads (10 kg and 12 kg) and for tablets of two different sizes ( $D = 9.85$  mm and  $D = 11.95$  mm). It is observed that the ratio of the side-weight-gain to top-weight-gain increases linearly with pan speed for the smaller tablets. For larger pan loads, the ratio of side-weight-gain to top-weight-gain increases with pan speed at a higher rate. However, for larger tablets, the variation is non-linear. This is because the tablets with curved sides can tumble more easily than tablets having a flat top and bottom surfaces. Thus the side is more exposed at higher pan speeds resulting in more side-weight-gain.

In order to elucidate and understand the dependence of  $CV(st)$  on the coating process time, we simulated the coating process for different coating times, from 10 min to 80 min. using the Monte Carlo technique. The variation of  $CV(st)$  with coating time also follows the same trend as for  $CV(tt)$ , namely  $CV(st)$  is proportional to  $t^{-0.5}$ , as shown in Fig. 17, for two different tablet sizes.

The dependence of  $CV(st)$  on the operational parameters (the pan speed, pan load, tablet size, and coating time) can be expressed as:

$$CV(st) = 1.87 \times 10^{-3} \frac{D^{1.49} N^{0.51}}{\omega^{0.54} t^{0.5} \varphi_s^{0.65}} \quad (11)$$

The comparison between  $CV(st)$  from the above model and by simulation is shown in Fig. 18.

For a uniform coating operation both the CVs should be minimum that gives equal coating on all the surfaces of a single tablet and also equal coating on all the tablets contained in a pan coater. Using the CV models, for a given set of tablets to be coated, the optimum parameters like speed or load of pan coater can be found. This data and methodology described here will be useful for the operation of the drum in a production environment, for evaluating the performance of the pan coater of different designs, for evaluating alternative hardware fitted inside the pan coater such as the shape, size, number



of baffles, the spray guns and the spray-distribution, and thereby for optimizing the operating parameters.

## 5. Conclusions

The Monte Carlo technique together with the data provided by the direct video imaging technique enables us to model and understand the role of the key process parameters rapidly. By introducing a “sphericity” term to account for the shape of the tablet in the model proposed earlier for the surface velocity and coating variation, we get a better fit to the experimental results. This data and methodology described here should be useful for the operation of the drum in a production environment, for evaluating the performance of the pan coater of different designs, for evaluating alternative hardware fitted inside the pan coater such as the shape, size, number of baffles, the spray guns and the spray-distribution, and thereby for optimizing the operating parameters.

Intuitively, a tablet with no sharp edges, i.e., a perfectly spherical tablet with sphericity = 1.0 should give the lowest CVs. To evaluate in detail just how significant an effect the sphericity has on CVs we would need to carry out further work on a range of tablets having the same values of  $D$  but different values of sphericity.

The video imaging technique described here should help to elucidate the role of all other process parameters that also need to be considered other than those already considered here, for example, the effect of different numbers or shapes of baffles fitted in the pan coater, the dynamics of the spray-droplets from the spray gun to the tablet surface, the size-distribution and concentration of the spray-droplets at the tablet surface and the actual spray-distribution over the tablet bed, particularly when more than one spray gun is used simultaneously in the pan coater. The dynamics of the spray process is a study by itself and will require a much higher optical resolution and a much faster camera in order to view individual drops striking, spreading and drying onto the surface of the tablets.

### Nomenclature

CCD	charge coupled device
CCTV	close circuit television
CV	coating variability
CV(st)	coating variability on a single tablet
CV(tt)	coating variability from tablet to tablet
HPMC	hydroxy propyl ethyl cellulose
ROI	region of interest
rpm	revolutions per minute
$A_{proj}$	projected area of tablet ( $\text{mm}^2$ )
$A_{proj}(j)$	projected area of tablet at $(x(j), y(j))$ ( $\text{mm}^2$ )
$A_{proj}(j+1)$	projected area of tablet at $(x(j+1), y(j+1))$ ( $\text{mm}^2$ )
$A_{total}$	total surface area of a single tablet ( $\text{mm}^2$ )
$D$	characteristic length of tablet (mm)
$d$	diameter of the tablet (mm)
$dt$	time increment (s)
$G$	mass flow rate (g/min)
$g$	acceleration due to gravity ( $\text{m/s}^2$ )
$H$	side thickness of tablet (mm)
$k$	proportionality constant
$m_i$	mass of tablet at $i^{\text{th}}$ iteration (g)
$m_{i+1}$	mass of tablet at $(i+1)^{\text{th}}$ iteration (g)
$N$	number of tablets
$N(i)$	tablet number at $i^{\text{th}}$ iteration
$R$	radius of pan (mm)
$S$	spray flux ( $\text{g/s/mm}^2$ )
$S(x, y)$	spray flux at any given point $(x, y)$ ( $\text{g/s/mm}^2$ )
$S_{max}$	maximum spray flux ( $\text{g/s/mm}^2$ )

$S_{min}$	minimum spray flux ( $\text{g/s/mm}^2$ )
$S(j)$	spray flux at $(x(j), y(j))$ ( $\text{g/s/mm}^2$ )
$S(j+1)$	spray flux at $(x(j+1), y(j+1))$ ( $\text{g/s/mm}^2$ )
$T$	total thickness of tablet (mm)
$t$	coating process time (min)
$t(i)$	coating process time at $i^{\text{th}}$ iteration (s)
$t_{circ}$	circulation time (s)
$t_{surf}$	surface time (s)
$t_{surf}(i)$	surface time at $i^{\text{th}}$ iteration (s)
$V_x$	velocity in X-direction (mm/s)
$V_y$	velocity of tablet parallel to the direction of tablets in cascading layer (velocity in Y-direction) (mm/s)
$W$	weight of tablet (g)
$x$	centroid X-location
$x(j)$	centroid X-location at $j^{\text{th}}$ iteration
$x(j+1)$	centroid X-location at $(j+1)^{\text{th}}$ iteration
$y$	centroid Y-location
$y(j)$	centroid Y-location at $j^{\text{th}}$ iteration
$y(j+1)$	centroid Y-location at $(j+1)^{\text{th}}$ iteration

### Greek letters

$\varphi_s$	sphericity of tablet
$\omega$	pan speed (1/s)
$v$	pan-load ratio
$\sigma(st)$	standard deviation of coating mass per unit surface area of a single tablet ( $\text{g/mm}^2$ )
$\sigma(tt)$	standard deviation of coating mass from tablet to tablet (g)
$\mu(st)$	mean of the coating weight gain distribution per unit area ( $\text{g/mm}^2$ )
$\mu(tt)$	mean of the coating weight gain distribution (g)
$\sigma_x$	standard deviation in X-direction
$\sigma_y$	standard deviation in Y-direction

## Acknowledgements

We would like to acknowledge the cooperation and the assistance extended to us by a) Mr. Manjrekar, the General Manager of Gansons Ltd. in making a production pan coater available to us for these experiments carried out in their production facility, and b) Mr. Sunil Tiwari, General Manager of Zydus Cadila Health Care Ltd., Thane, in providing us with the uncoated and coated tablets as well as the facilities to carry out a part of the spray-coating experiments in their production facility.

## Appendix

### Derivation of spray flux distribution

The simplifying assumptions that we have made in calculating the spray dynamics in a pan-coating process are:

- The spray flux is distributed normally (in both X and Y directions) over all of the spray region. This implies that a single spray gun is used.
- The spray pattern is assumed to be a rectangle (with dimensions of  $210 \text{ mm} \times 190 \text{ mm}$ ), although in practice it is more of an elliptical shape.
- The ratio of maximum to minimum spray flux over the spray region is 0.75.
- 25% of the coating material is lost between the spray gun and the tablet due to the hot dry air.

The spray flux is defined as the amount of coating material sprayed per unit area per unit time. If we consider it to have a bi-

variate normal distribution with mean at '0', it can be expressed as Eq. A1:

$$S(x,y) = \frac{1}{2\pi\sigma_x\sigma_y} \exp\left(\frac{-1}{2}\left(\frac{x^2}{\sigma_x^2} + \frac{y^2}{\sigma_y^2}\right)\right) \quad (\text{A1})$$

where  $\sigma$  is the variance and the subscripts indicate the direction.

The coating material used is HPMC, and the density of 10% aqueous HPMC is 1035 kg/m<sup>3</sup>. Typical values of the flow rate and dilution ratio (w/w) of coating material are 125 ml/min and 0.1 respectively. From the above data amount of coating material sprayed over total spray region is calculated and this is also calculated by integrating spray flux over the total spray region gives Eq. A2:

$$\int_{-105}^{105} \int_{-85}^{85} \frac{1}{2\pi\sigma_x\sigma_y} \exp\left(\frac{-1}{2}\left(\frac{x^2}{\sigma_x^2} + \frac{y^2}{\sigma_y^2}\right)\right) = 0.16 \text{ g/s.} \quad (\text{A2})$$

The spray flux is a maximum ( $S_{max}$ ) at the centre of the rectangle, that is at (0, 0). The minimum of spray flux ( $S_{min}$ ) is at the corners of the rectangle, which is at (105, 85), (−105, 85), (−105, −85) and (105, −85).

Simplifying the assumption-(c) we get:

$$\exp\left(\frac{-1}{2}\left(\frac{105^2}{\sigma_x^2} + \frac{85^2}{\sigma_y^2}\right)\right) = 0.75. \quad (\text{A3})$$

The variances in two directions are obtained by solving the Eqs. A2 and A3.

Thus the spray flux Eq. A1 now becomes

$$S(x,y) = \frac{1}{2\pi(195)(163)} \exp\left(\frac{-1}{2}\left(\frac{x^2}{195^2} + \frac{y^2}{163^2}\right)\right). \quad (\text{A4})$$

## References

- [1] U. Mann, M. Rubinovitch, E.J. Crosby, Challenges in the modeling and prediction of coating of pharmaceutical dosage forms, *AIChE Journal* 25 (1979) 873–882.
- [2] C. Denis, M. Hemati, D. Chulia, J.-Y. Lanne, B. Buisson, G. Daste, F. Elbaz, A model of surface renewal with application to the coating of pharmaceutical tablets in rotary drums, *Powder Technology* 130 (2003) 174–180.
- [3] R.Y. Yang, R.P. Zou, A.B. Yu, Micro dynamic analysis of particle flow in a horizontal rotating drum, *Powder Technology* 130 (2003) 138–146.
- [4] Y. Song, R. Turton, F. Kayihan, Contact detection algorithms for DEM simulations of tablet-shaped particles, *Powder Technology* 161 (2006) 32–40.
- [5] P. Pandey, Y. Song, F. Kayihan, R. Turton, Simulation of particle movement in a pan coating device using discrete element modeling and its comparison with video-imaging experiments, *Powder Technology* 161 (2006) 79–88.
- [6] S. Sandadi, P. Pandey, R. Turton, In-situ, near real-time acquisition of particle motion in rotating pan coating equipment using imaging techniques, *Chemical Engineering Science* 59 (2004) 5807–5817.
- [7] P. Pandey, R. Turton, Movement of different-shaped particles in a pan-coating device using novel video-imaging techniques, *AAPS PharmSciTech* 6 (2005) 237–244.
- [8] R. Muller, P. Kleinebudde, Prediction of tablet velocity in pan coaters for scale-up, *Powder Technology* 173 (2007) 51–58.
- [9] D. Cahn, D. Fuerstenau, Simulation of diffusional mixing of particulate solids by Monte Carlo techniques, *Powder Technology* 1 (1967) 174–182.
- [10] P. Pandey, M. Katakdaunde, R. Turton, Modeling weight variability in a pan coating process using Monte Carlo simulations, *AAPS PharmSciTech* 7 (4) (2006) Article 83.
- [11] K. KuShaari, P. Pandey, Y. Song, R. Turton, Monte Carlo simulation to determine coating uniformity in a Wurster fluidized bed coating process, *Powder Technology* 166 (2006) 81–90.
- [12] R. Turton, Challenges in the modeling and prediction of coating of pharmaceutical dosage forms, *Powder Technology* 181 (2008) 186–194.
- [13] G.W. Smith, G.S. Macleod, J.T. Fell, Mixing efficiency in side-vented coating equipment, *AAPS PharmSciTech* 4 (2003) 1–5.